Applied Energy 210 (2018) 974–986

Contents lists available at ScienceDirect

Applied Energy

journal homepage: www.elsevier.com/locate/apenergy

Optimal coordinated energy dispatch of a multi-energy microgrid in grid-connected and islanded modes

Zhengmao Li, Yan Xu*

School of Electrical and Electronic Engineering, Nanyang Technological University, 50 Nanyang Avenue, 639798, Singapore

ARTICLE INFO

Keywords:
Multi-energy microgrids
Combined cooling
Heat and power plant
System–wide optimal coordinated dispatch
Mixed-integer linear programming
Net operating cost

ABSTRACT

This paper proposes a system-wide optimal coordinated energy dispatch method for a multi-energy microgrid in both the grid-connected and islanded modes. The studied microgrid consists of multiple energy carriers covering the controllable generation units (fuel cell, electric boiler, combined cooling, heat and power plant and electric chiller), uncontrollable generation units (wind turbine and photovoltaic cell) and energy storage devices (battery storage, heat storage tank and ice storage tank). The proposed energy dispatch method aims to minimize the microgrid net operating cost and enhance the dispatch flexibility in supplying power, heat and cooling in the day-ahead energy market. For both the grid-connected and islanded microgrid, their dispatch models are formulated as the mixed-integer linear programming problems, which can be efficiently solved by the commercial solvers. Comprehensive case studies are performed to evaluate the effectiveness of the proposed method and then compared with the traditional dispatch methods which supply power and heat/cooling energies separately. Simulation results demonstrate that the proposed method can achieve much higher operating efficiency.

1. Introduction

Multi-energy systems aim to integrate diverse energy carriers such as electricity, heat and cooling, to achieve higher energy utilization efficiency [1]. In practice, the multiple energies can be simultaneously generated by highly efficient co- or tri-generation units such as the combined cooling, heat and power (CCHP) plant [2,3]. Once deployed in the distribution network, the CCHP plant, energy storage and the renewable energy-based distributed generation (DG) units such as solar and wind power can form a multi-energy microgrid [2–4]. Therefore, one key research problem is to optimally dispatch multi-energy related units for the maximum operating efficiency.

In the literature about the multi-energy integration, most of the research works focus on the operation at the individual CCHP plants level, which can generally fall into two strategies, *i.e.*, following power load (FPL) and following heat load (FHL) strategy [5–10]. Fang et al. [5] worked on the FPL/FHL switching strategies to enhance the integrated performance of energy consumption, operating cost and CO_2 emissions of the CCHP plant. Similarly, to minimize the excess power or heat energy produced by the CCHP plant, Smith et al. [6] compared the FPL and FHL with a hybrid strategy which either followed FPL or FHL strategy. In [7] and [8], operational strategies for CCHP plant were designed for different operational conditions and corresponding evaluation criteria. With a ground source heat pump, Kang et al. [9] configured a CCHP-organic Rankine cycle system and analyzed its performance in the cost savings, gas emission reduction, and system efficiency improvement. In [10], matrix modelling approach was introduced to optimize the input and output power of CCHP plant as well as its capacity. Although many research works have been done on the operation of the single CCHP plant, its coordination with other DGs to supply multiple energies at a system level (*e.g.*, microgrid) was not systematically studied.

At the microgrid level, most of the current research works focus only on the operation of single-energy microgrids [11–13], which do not integrate multiple energies. Further, the research works on the coordination of the CCHP plant with other DGs in supplying multiple energies are mainly for the grid-connected microgrids [14,15]. Ma et al. [16] investigated the coordination of the CCHP plant and photovoltaic prosumers to minimize the operating cost in a grid-connected microgrid. In [17], the robust optimization method was employed to coordinate the CCHP plant with DGs of uncertain outputs to handle the intermittency. Wang et al. [18] proposed an integrated multi-objective dispatch method for the microgrid to minimize its net operating cost and gas emissions. In [19], an optimization method for the operation and design of microgrid with power and heat demands was proposed considering the uncertainty of renewable energies. In our recent work [20], the dynamic dispatch method for a grid-connected multi-energy microgrid considering the opportunity profit by the electrical energy

* Corresponding author.
E-mail address: XUYAN@ntu.edu.sg (Y. Xu).

http://dx.doi.org/10.1016/j.apenergy.2017.08.197
Received 31 May 2017; Received in revised form 12 August 2017; Accepted 24 August 2017
Available online 31 August 2017

Nomenclature

Sets and indices

t set of dispatch time, running from 1 to N
j set of CG, running from 1 to N_{CG}
k set of the blocks, running from 1 to N_L
m set of the units, including WT, PV, MT, FC, EB, EC and ES, running for 1 to N_U

Variables and parameters

η_{MT}^t/η_{FC}^t electrical efficiency of MT/FC
P_{MT}^t/P_{FC}^t power outputs of MT/FC
Q_{MTH}^t/Q_{MTC}^t heat/cooling outputs of MT
η_H/η_C heat recovery ratio of the heat recovery unit/absorption chiller
COP_H/COP_C coefficient of performance of heat recovery unit/absorption chiller
η_L heat loss ratio of MT
E_{ES}^t energy stored in ES
P_{ESC}^t/P_{ESD}^t charging/discharging power of ES
τ_{ES} decay rate of ES
η_{ESC}/η_{ESD} charging/discharging rates of ES
Q_{EB}^t/Q_{EC}^t heat/cooling outputs of EB/EC
P_{EB}^t/P_{EC}^t power inputs of EB/EC
COP_{EB}/COP_{EC} heat/cooling coefficient of performance of EB/EC
F_G/F_S net operating cost of the grid-connected/islanded microgrid
C_{CP} capital cost
$C_{CP,m}/n_m$ initial investment cost/life span of unit m
l annual interest rate
C_F^t/C_{OM}^t fuel/maintenance cost
C_{EX}^t/C_{PH}^t power exchange/energy deviation cost
C_{ST}^t/C_{SD}^t start-up/shut-down cost
C_{HC}^t/C_{SHC}^t revenue of supplying heat/cooling in grid-connected/islanded microgrid
$C_{F,FC}^t/C_{F,MT}^t$ fuel cost of FC/MT
c_G/L_{NG} unit price/lower heating value of natural gas
P_{WT}^t/P_{PV}^t power outputs of WT/PV
K_{WT}^{om}/K_{PV}^{om} unit maintenance cost of WT/PV
$K_{EC}^{om}/K_{EB}^{om}/K_{MT}^{om}$ unit maintenance cost of EC/EB/MT
K_{FC}^{om}/K_{ES}^{om} unit maintenance cost of FC/ES
$C_{ST,j}^U/C_{SD,j}^D$ unit start-up/shut-down cost of unit j
P_B^t/P_S^t purchasing/selling power of microgrid
c_B^t/c_S^t unit power purchasing/selling price of microgrid
C_H^t/C_C^t revenue of supplying heat/cooling in grid-connected microgrid
c_H/c_C unit price of supplying heat/cooling to customers
P_{BSC}^t/P_{BSD}^t charging/discharging power of BS
P_{ISTC}^t/P_{ISTD}^t absorbing/releasing power of IST
P_{HSTC}^t/P_{HSTD}^t absorbing/releasing power of HST
Q_H^t/Q_C^t heat/cooling demands of microgrid
P_L^t power demands of microgrid
U_j^t binary status of unit j, $U_j^t = 1$ is on, 0 is off
$P_{CG,j}^t$ power of controllable unit j
$P_{CG,j}^{min}/P_{CG,j}^{max}$ minimum/maximum power of unit j
$R_{CG,j}^{up}/R_{CG,j}^{down}$ maximum ramp up/down rate of unit j
P_B^{max}/P_S^{max} maximum purchasing/selling power of microgrid
γ_B^t/γ_S^t binary state variables with $\gamma_B^t = 1/\gamma_S^t = 1$, microgrid purchases/sells power
$P_{ESC}^{max}/P_{ESD}^{max}$ maximum charging/discharging power of ES
$\gamma_{ESC}^t/\gamma_{ESD}^t$ binary state variables with $\gamma_{ESC}^t = 1/\gamma_{ESD}^t = 1$, ES is charging/discharging
$\xi_{ES}^{min}/\xi_{ES}^{max}$ minimum/maximum state of charge of ES
Cap_{ES} capacity of ES
$c_{TE}/c_{IE}/c_{DE}$ unit cost for heat/cooling/power surplus
$c_{TS}/c_{IS}/c_{DS}$ unit cost for heat/cooling/power shortage
$Q_{TS}^t/Q_{IS}^t/P_{DS}^t$ heat/cooling/power shortage
$Q_{TE}^t/Q_{IE}^t/P_{DE}^t$ heat/cooling/power surplus
C_{SH}^t/C_{SC}^t revenue of supplying heat/cooling in islanded microgrid
$\gamma_{TS}^t/\gamma_{IS}^t/\gamma_{DS}^t$ binary indicators of heat/cooling/power shortage, 1 means that there is energy shortage
$\gamma_{TE}^t/\gamma_{IE}^t/\gamma_{DE}^t$ binary indicators of the heat/cooling/power surplus,1 means that there is energy surplus
α_k/β_k slope/intercept of linear function in block k
P_k starting point of kth block
P_1/P_{N+1} minimum/maximum power outputs of N_L blocks
Δt unit dispatch interval, 1 h
B_k^t binary state of block k
P_k^t general power output of MT or FC
$C_{U,FC}^t/C_{U,PG}^t$ unit power generation cost of FC/MT for only power generation
$C_{U,S}^t/C_{U,W}^t$ unit power generation cost of MT in summer/winter

storage was studied to increase the system operating efficiency.

Much work has been done on the operation of grid-connected microgrids in the literature, but very few research works consider the multi-energy dispatch of the islanded operating modes. Besides, the existing related works on the dispatch of islanded microgrids still focus on its single-energy dispatch only, *i.e.*, the power dispatch of the islanded microgrids [11,12,21–23]. In practice, the multi-energy management of the islanded microgrids is important especially for some remote areas like the Semakau Island microgrid in Singapore [4]. Without the grid as the backup, the operation objective of the islanded microgrids is rather different from the grid-connected ones. The research work in [24] is one of the few studies which proposed a multi-objective optimization method for the minimization of the fuel cost and gas emission.

It can be observed that for the operation of individual CCHP plant, all the above works adopt the FPL/FHL or hybrid of the two strategies; while at the system level, CCHP plant typically operates under the FHL strategy in grid-connected microgrids since the power imbalance can be compensated by the grid, for the islanded microgrids, the FPL strategy for CCHP plant is preferred in that the power system requires a precise power balance all the time but the imbalance of the heat/cooling energy for short periods is acceptable [14]. However, under the above strategies, power and heat/cooling outputs of the CCHP plant are highly coupled and dependent on one another, which makes the microgrid operation not flexible enough and the potentials of CCHP plant in the system cost saving are not fulfilled.

Moreover, given the nonlinear nature of the dispatch problem, the solution methods are mostly the evolutionary algorithms like the Genetic Algorithm or Particle Swarm Optimization [12,14,16–18,21,24]. However, these algorithms are computationally demanding, especially when the problem dimension is high. Further, they often suffer from issues such as the inconsistent solutions and difficult to rigorously converge. Since the new competitive environment in the power system requires more accurate and efficient tools to support decisions for the resource dispatch, more efficient solution process and quality are needed [25].

This paper studies on a comprehensive multi-energy microgrid which consists of a CCHP plant, a battery storage (BS), an electric chiller (EC), a heat storage tank (HST), a wind turbine (WT), a photovoltaic cell (PV), an ice storage tank (IST), an electric boiler (EB) and a fuel cell (FC). To achieve higher dispatch flexibility and operating efficiency, the system-wide optimal coordinated dispatch models for microgrid under both grid-connected and islanded modes are proposed. In the models, the HST and IST are utilized to decouple the inflexible

operational strategies of the CCHP plant, and then the power and heat/cooling outputs of the CCHP plant can participate in the day-ahead energy market with higher flexibility. The conversion units, *i.e.*, the EB and EC, which transfer power to heat/cooling, can further enhance the coordination of different energies. The objectives are to minimize the net operating cost of the microgrid in both modes subject to the system operational limits. Besides, the nonlinear dispatch models are linearized to the mixed-integer linear programming (MILP) ones for higher solution efficiency and quality. Finally, typical scenarios of the winter and summer days are used to fully test the validity of the proposed dispatch method.

The aim of this paper can be summarized as: firstly, increase the system operating efficiency and dispatch flexibility via the coordination of different DGs, energy storage devices as well as the demand response; secondly, make full use of the pricing schemes and enhance the interaction of multiple energies at the system level; finally, reflect the practical operational condition through the detailed and practical modelling and improve the solution efficiency and quality by the linearization. Compared with the existing research works on multi-energy microgrid dispatch, major contributions of this paper can be summarized as:

1. A coordinated day-ahead energy dispatch method for the multi-energy microgrid is proposed for both grid-connected and islanded modes. The method considers a comprehensive set of practical components for realistic multi-energy microgrid operation.
2. The conventional inflexible operational strategies (FPL/FHL) of CCHP plant are decoupled. Without the coupling limits, the CCHP plant can join in the whole energy market with higher flexibility. Then the operation of CCHP plant with other DGs as well as multiple energy resources is further coordinated at the microgrid level.
3. The nonlinear dispatch problems are linearized to MILP models which can be efficiently solved by the commercial solvers. Compared with evolutionary algorithms, the solution quality and speed can be ensured for online application.

The rest of this paper is organized as follows. System description and modelling are given in Section 2. In Section 3, the coordinated dispatch models of a multi-energy microgrid in both modes are introduced. Case studies are presented and analyzed in Section 4. Then the paper is ended with some conclusions in Section 5.

2. Multi-energy microgrid modelling

In this study, the multi-energy microgrid consists of a wind turbine, a photovoltaic cell, a battery storage, a CCHP plant, a fuel cell, an electric boiler, a heat storage tank, an electric chiller and an ice storage tank as shown in Fig. 1. Besides, there is a switch between the grid and microgrid: when the switch is on, the microgrid operates in the grid-connected mode; while off, the microgrid operates in the islanded mode [21–23].

The components modelling mainly focuses on their external characteristics, *i.e.*, their ON/OFF statuses as well as generation outputs [15]. The detailed models are given in the following subsections. It should be noted that the internal characteristics of each component are neither the focus nor necessary for the energy dispatch problem as studied in this paper. Thus, they are not reflected in the modelling part. Besides, for the micro-turbine (or the CCHP plant), electric boiler, fuel cell, and electric chiller are of the small sizes, flexible control and fast start-up/shut-down rates, hence, they can be regarded as the controllable generation (CG) units; while WT and PV whose power outputs are uncertain and volatile are categorized as the uncontrollable generation units.

2.1. CCHP plant

Typically, the CCHP plant consists of three parts: a micro-turbine (MT), an absorption chiller and a heat recovery unit. MT consumes natural gas to generate power, at the same time, the waste heat can be utilized by the heat recovery unit/absorption chiller to produce heat/cooling energy [5,19]. Thus the energy utilization efficiency can be greatly improved. In this paper, the Capstone's micro-turbine C65 [26], which has a high international market share, is used as the reference for the modelling of CCHP plant. The relation between the power outputs and electrical efficiency can be modeled as

$$\eta_{MT}^{t} = 2.767 \times 10^{-7}(P_{MT}^{t})^{3} - 7.337 \times 10^{-5}(P_{MT}^{t})^{2} + 6.385 \times 10^{-3}P_{MT}^{t} + 0.107 \quad (1)$$

where t is the current dispatch time; η_{MT}^{t} and P_{MT}^{t} denote electrical

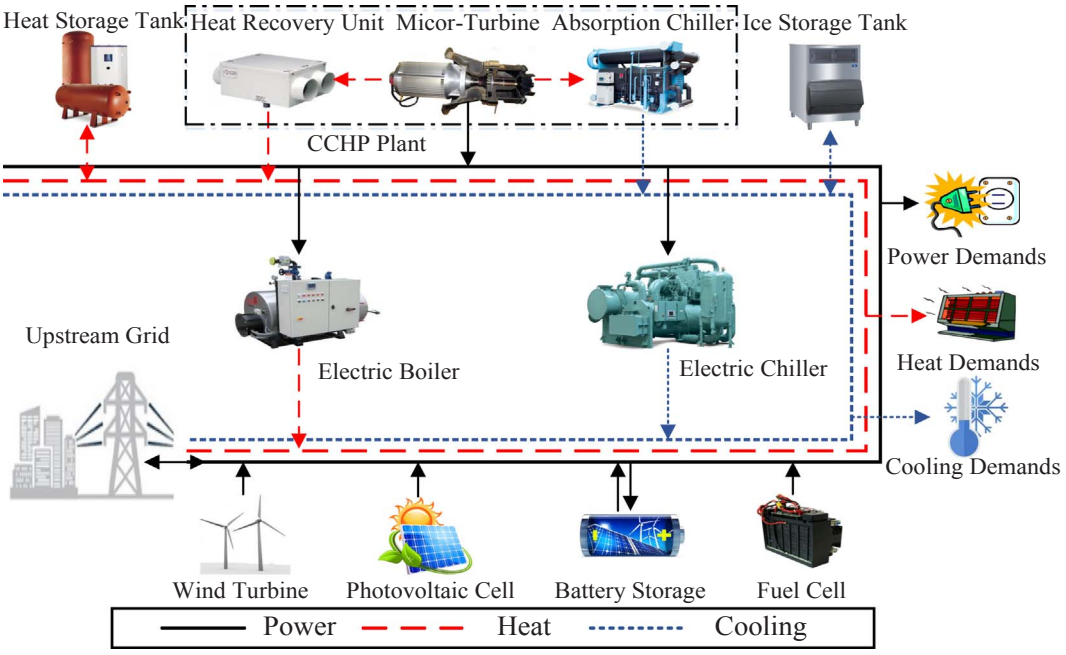

Fig. 1. Structure of a multi-energy microgrid.

efficiency and power outputs of MT respectively.

The corresponding heat and cooling outputs are

$$Q_{MTH}^t = \eta_H COP_H P_{MT}^t (1-\eta_{MT}^t-\eta_L)/\eta_{MT}^t \quad (2)$$

$$Q_{MTC}^t = \eta_C COP_C P_{MT}^t (1-\eta_{MT}^t-\eta_L)/\eta_{MT}^t \quad (3)$$

where η_H, η_C and COP_H, COP_C denote heat recovery ratio and coefficient of performance of heat recovery unit and absorption chiller; η_L is heat loss ratio; Q_{MTH}^t and Q_{MTC}^t are heat and cooling outputs, respectively.

Both the heat and cooling energy come from the waste heat, thus, they share similar properties. If the waste heat is not recovered, MT operates only for the power generation [12,27,28].

2.2. Energy storage

Energy storage (ES) can decouple the energy generation from its consumption as well as reduce the imbalance between the energy supply and demand [29]. In this paper, energy storage mainly consists of three types: electric energy storage, heat storage, and cooling storage.

(1) Electrical energy storage: currently, the electrical energy storage including the power-type like the supercapacitors and energy-type like electrochemical batteries, is intensively investigated. The power-type energy storage is mostly utilized to alleviate the effects from the fluctuating outputs of renewable energy generators on the power system operation, while the energy-type energy storage is mainly used for the peak shaving in the energy management field [30]. For the day-ahead energy dispatch scheme in this paper, battery storage, an energy-type storage is applied [20,31].

(2) Heat/cooling storage: under the FHL/FPL strategies, the power or heat/cooling outputs of CCHP plant are limited by one another, which reduces the operational flexibility of the CCHP plant in the overall multi-energy dispatch. To decouple the inflexible operational strategies, the heat storage tank and ice storage tank, whose operational principles are similar to the electrical energy storage are deployed in the microgrid. Nowadays, the HST and IST have already been widely employed in European nations like Denmark [32], and they also have a great application prospect in other regions with multi-energy supply and demand.

Since the models for IST/HST and BS are similar, in this study, ES is used as the generalized abbreviation to demonstrate the relationship between their energy and power as below. In practice, ES should be BS, HST or IST.

$$E_{ES}^t = (1-\tau_{ES})E_{ES}^{t-1} + (P_{ESC}^t \eta_{ESC} + P_{ESD}^t/\eta_{ESD})\Delta t \quad (4)$$

where η_{ESC} and η_{ESD} are the charging and discharging rates; P_{ESC}^t and P_{ESD}^t denote the charge and discharge power of ES; τ_{ES} is the decay rate; E_{ES}^t denotes the energy in energy storage at time t; Δt is the unit dispatch interval.

2.3. Electric boiler and electric chiller

To enhance the interaction of different energy systems, the electric boilers (EB) and electric chillers (EC) are utilized to convert power into heat/cooling. It should be noted that different types of EB/EC share the similar operating models as below, thus in this paper, the EB/EC is not limited to a specific type [17].

$$Q_{EB}^t = P_{EB}^t COP_{EB} \quad (5)$$

$$Q_{EC}^t = P_{EC}^t COP_{EC} \quad (6)$$

where P_{EB}^t and P_{EC}^t denote power inputs of EB and EC; COP_{EB}, COP_{EC} and Q_{EB}^t,Q_{EC}^t are the heat and cooling coefficient of performance and outputs of EB and EC.

2.4. Fuel cells

Fuel cells (FC) can convert the energy stored in O_2 and H_2 into the pollution-free electrical energy by an electrochemical process [33]. Due to the high electrical efficiency, the waste heat of FC is not recovered [12,20,34]. In this study, the proton-exchange membrane fuel cell IFC PC-29, powered by natural gas [35], is chosen as a reference, the relation between its electrical efficiency and power outputs can be given by

$$\eta_{FC}^t = -0.0023 P_{FC}^t + 0.674 \quad (7)$$

where η_{FC}^t and P_{FC}^t denote the electrical efficiency and power outputs of FC at time t.

Note that the power generation models for WT and PV are widely applied in the power system dispatch problems, one can refer to reference [36,37] for the specific details.

3. Optimal coordinated dispatch

With regard to the different microgrid operating modes, the system-wide coordinated dispatch models are proposed respectively in this paper.

3.1. Grid-connected mode

In the grid-connected microgrid, the power imbalance can be all compensated by the grid, *i.e.*, no power surplus or shortage will appear. Thus the objective is to minimize the net operating cost F_G [27].

(1) Objective function:

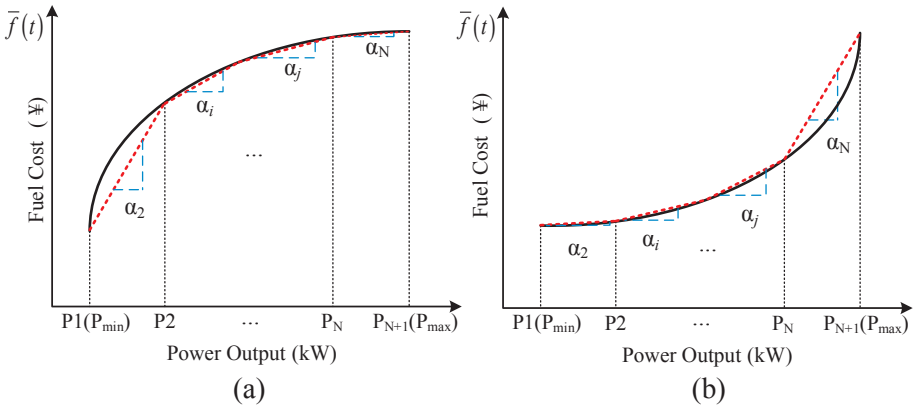

Fig. 2. Piecewise linearization of the nonlinear items. (a) fuel cost of the CCHP plant or FC, (b) heat or cooling outputs of CCHP plant.

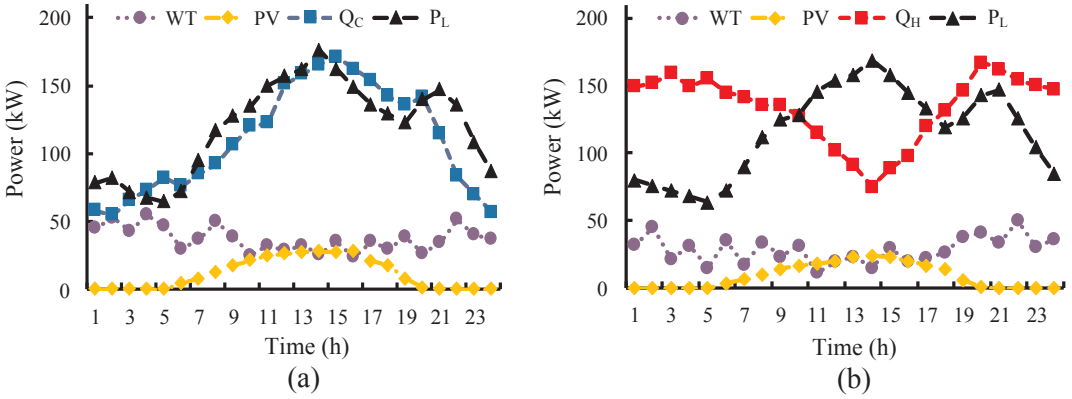

Fig. 3. Forecasted loads, PV and WT power outputs. (a) Summer, (b) Winter.

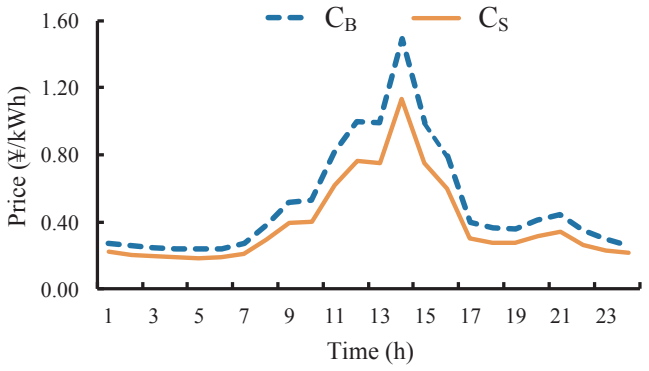

Fig. 4. The real-time pricing scheme.

$$MIN\ F_G = C_{CP} + \sum_{t=1}^{N} (C_F^t + C_{EX}^t + C_{OM}^t + C_{ST}^t + C_{SD}^t - C_{HC}^t)\Delta t \tag{8}$$

(a) Capital cost C_{CP} [38]:

$$C_{CP} = \sum_{m=1}^{N_U} C_{CP,\,m}\, l(1+l)^{n_m}/[(1+l)^{n_m}-1] \tag{9}$$

(b) Fuel cost C_F^t:

$$C_F^t = C_{F,FC}^t + C_{F,MT}^t = [c_G(P_{MT}^t/\eta_{MT}^t + P_{FC}^t/\eta_{FC}^t)]/L_{NG} \tag{10}$$

(c) Maintenance cost C_{OM}^t:

$$C_{OM}^t = P_{EC}^t \cdot K_{EC}^{om} + P_{WT}^t \cdot K_{WT}^{om} + P_{PV}^t \cdot K_{PV}^{om} + P_{EB}^t \cdot K_{EB}^{om} + P_{MT}^t \cdot K_{MT}^{om} + P_{FC}^t \cdot K_{FC}^{om} + (P_{ESC}^t + P_{ESD}^t) \cdot K_{ES}^{om} \tag{11}$$

(d) Start-up cost C_{ST}^t and C_{SD}^t shut-down cost:

$$C_{ST}^t = \sum_{j=1}^{N_{CG}} \max\{0, U_j^t - U_j^{t-1}\} C_{ST,j}^U \tag{12}$$

$$C_{SD}^t = \sum_{j=1}^{N_{CG}} \max\{0, U_j^{t-1} - U_j^t\} C_{SD,j}^D \tag{13}$$

(e) Power exchange cost C_{EX}^t:

$$C_{EX}^t = c_B^t P_B^t - c_S^t P_S^t \tag{14}$$

(f) Revenue of supplying heat and cooling C_{HC}^t:

$$C_{HC}^t = C_H^t + C_C^t = c_H Q_H^t + c_C Q_C^t \tag{15}$$

where N is the total number of the dispatch periods; m denotes the index of the units, and m can be WT, PV, MT, FC, EB, EC and ES; N_U is the number of the DGs and ES; $C_{CP,m}$ and n_m denote the initial investment cost and the life span of unit m; l is the annual interest rate; c_G and L_{NG} denote the unit price and lower heating value of natural gas; $K_{EC}^{om}, K_{WT}^{om}, K_{PV}^{om}, K_{EB}^{om}, K_{MT}^{om}, K_{FC}^{om}$ and K_{ES}^{om} are the unit maintenance cost of EC, WT, PV, EB, MT, FC, ES, HST and IST; N_{CG} and j are the number and index of controllable units (MT, FC, EB and EC); $C_{F,FC}^t$ and $C_{F,MT}^t$ denote the fuel cost of MT and FC respectively; U_j^t denotes the binary status of unit j, $U_j^t = 1$ means the unit is on, 0 is off; $C_{ST,j}^U$ and $C_{SD,j}^D$ are the unit start-up and shut-down cost of unit j; P_B^t and P_S^t are the purchasing and selling power of microgrid; c_B^t and c_S^t denote the unit power purchasing and selling price; Q_H^t and Q_C^t denote the heat and cooling loads; c_H and c_C are the unit price of supplying heat and cooling to customers; C_H^t and C_C^t denote the heat and cooling selling revenue respectively.

(2) Constraints

The operational constraints include the following [28,31]:

(a) Energy balance:

$$P_{WT}^t + P_{PV}^t + P_{MT}^t + P_{FC}^t + P_{BSD}^t - P_{BSC}^t + P_B^t - P_S^t = P_L^t + P_{EB}^t + P_{EC}^t \tag{16}$$

$$Q_{EC}^t + Q_{MTC}^t - P_{ISTC}^t + P_{ISTD}^t = Q_C^t \tag{17}$$

$$Q_{EB}^t + Q_{MTH}^t - P_{HSTC}^t + P_{HSTD}^t = Q_H^t \tag{18}$$

(b) Controllable units:

Table 1
Parameters of energy storage [5,7,8].

Type	η_C/η_D	τ_{ES}	P_{ESC}^{max}	P_{ESD}^{max}	ξ_{min}	ξ_{max}	K_{ES}^{om}/(¥/kW h)	E_{ES}^0	Cap_{ES}	$C_{CP,ES}$/(¥/kW)	n_{ES}/yr
BS	90%	0.001	37.5	37.5	0.2	0.8	0.0073	30	150	670	10
HST	87%	0.01	45	45	0	0.9	0.0012	0	160	450	20
IST	85%	0.01	40	40	0	0.9	0.0014	0	120	450	20

Table 2
Parameters of DGs [38,43,44].

Type	$C_{CP,m}$/(¥/kW)	n_m/yr	P_m^{min}	P_m^{max}	$C_{ST,m}^U$	$C_{SD,m}^U$	R_m^{up}	R_m^{down}	K_m^{om}
MT	10000	25	15	65	1.94 ¥	1.82 ¥	10 kW/min	5 kW/min	0.0990 ¥/kW h
FC	29000	20	0	40	2.21 ¥	2.05 ¥	2 kW/min	2 kW/min	0.0841 ¥/kW h
WT	11000	20	0	55	–	–	–	–	0.0145 ¥/kW h
PV	2000	25	0	30	–	–	–	–	0.0133 ¥/kW h
EB	1000	15	0	50	1.23 ¥	1.14 ¥	3 kW/min	2 kW/min	0.0089 ¥/kW h
EC	1000	15	0	41	1.32 ¥	1.15 ¥	4 kW/min	3 kW/min	0.0104 ¥/kW h

Table 3
value of parameters [10,11,27].

Parameters	Value	Parameters	Value	Parameters	Value	Parameters	Value
COP_H	1.2	C_{TS}	0.20 ¥/kW h	C_{DS}	1.50 ¥/kW h	η_H/η_C	85%
COP_C	2	C_{TE}	0.15 ¥/kW h	C_{DE}	0.90 ¥/kW h	η_L	15%
COP_{EB}	0.85	C_{IS}	0.12 ¥/kW h	C_G	2.70 ¥/m^3	C_H	0.30 ¥/kW h
COP_{EC}	3.5	C_{IE}	0.10 ¥/kW h	L_{NG}	9.78 kW h/m3	C_C	0.20 ¥/kW h

Table 4
combination of all the units in three cases.

No.	Common units				Summer			Winter		
	PV/WT	FC	BS	MT	GB	EC	IST	GB	EB	HST
Case 1	√	√	√	√	√			√		
Case 2	√	√	√	√	√			√		
Case 3	√	√	√	√		√	√		√	√

Power output limit: $U_j^t \cdot P_{CG,j}^{min} \le P_{CG,j}^t \le U_j^t \cdot P_{CG,j}^{max}$ (19)

Ramp up/down limit: $R_{CG,j}^{down}\Delta t \le P_{CG,j}^t - P_{CG,j}^{t-1} \le R_{CG,j}^{up}\Delta t$ (20)

(c) Power exchanges:

Power exchange limit: $0 \le P_B^t \le \gamma_B^t P_B^{max}, 0 \le P_S^t \le \gamma_S^t P_S^{max}$ (21)

State limit: $\gamma_B^t + \gamma_S^t \le 1$ (22)

(d) Energy storage:

Charging power limit: $0 \le P_{ESC}^t \le \gamma_{ESC}^t P_{ESC}^{max}$ (23)

Discharging power limit: $0 \le P_{ESD}^t \le \gamma_{ESD}^t P_{ESD}^{max}$ (24)

Energy limit: $\xi_{ES}^{min} Cap_{ES} \le E_{ES}^t \le \xi_{ES}^{max} Cap_{ES}$ (25)

Starting/ending energy limit: $E_{ES}^0 = E_{ES}^{N\Delta t}$ (26)

State limit: $\gamma_{ESC}^t + \gamma_{ESD}^t \le 1$ (27)

where P_{WT}^t and P_{PV}^t are the power output of WT and PV; P_L^t is the power demands; $P_{CG,j}^t$ denotes the power of controllable unit j; $P_{CG,j}^{min}$ and $P_{CG,j}^{max}$ are the minimum and maximum power of unit j; $R_{CG,j}^{up}$ and $R_{CG,j}^{down}$ are the maximum ramp up/down rate of unit j; γ_B^t and γ_S^t are binary state variables, when $\gamma_B^t = 1$, the microgrid purchases power from grid, when $\gamma_S^t = 1$, microgrid sells power; γ_{ESC}^t and γ_{ESD}^t are binary state variables with $\gamma_{ESC}^t = 1$ indicating that ES is charging and $\gamma_{ESD}^t = 1$ is discharging; P_{ESC}^{max} and P_{ESD}^{max} are the maximum charge and discharge power; ξ_{ES}^{min} and ξ_{ES}^{max} denote the ES's minimum and maximum state of charge; Cap_{ES}, E_{ES}^0 and $E_{ES}^{N\Delta t}$ are the capacities, starting and ending energy of ES; P_{BSC}^t and P_{BSD}^t denote the charge and discharge power of BS; P_{HSTC}^t,P_{HSTD}^t and P_{ISTC}^t,P_{ISTD}^t denote the absorbing and releasing power of HST and IST respectively.

Note that CG is a generalized abbreviation which includes MT, EB, EC and FC.

3.2. Islanded mode

Without the grid as the backup, the energy generation and consumption should be balanced within the islanded microgrid. In this

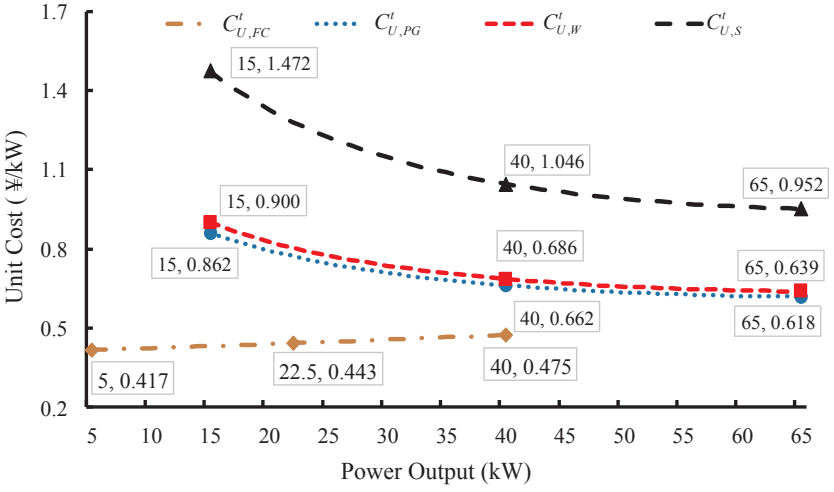

Fig. 5. Unit power generation cost of FC and MT in different modes.

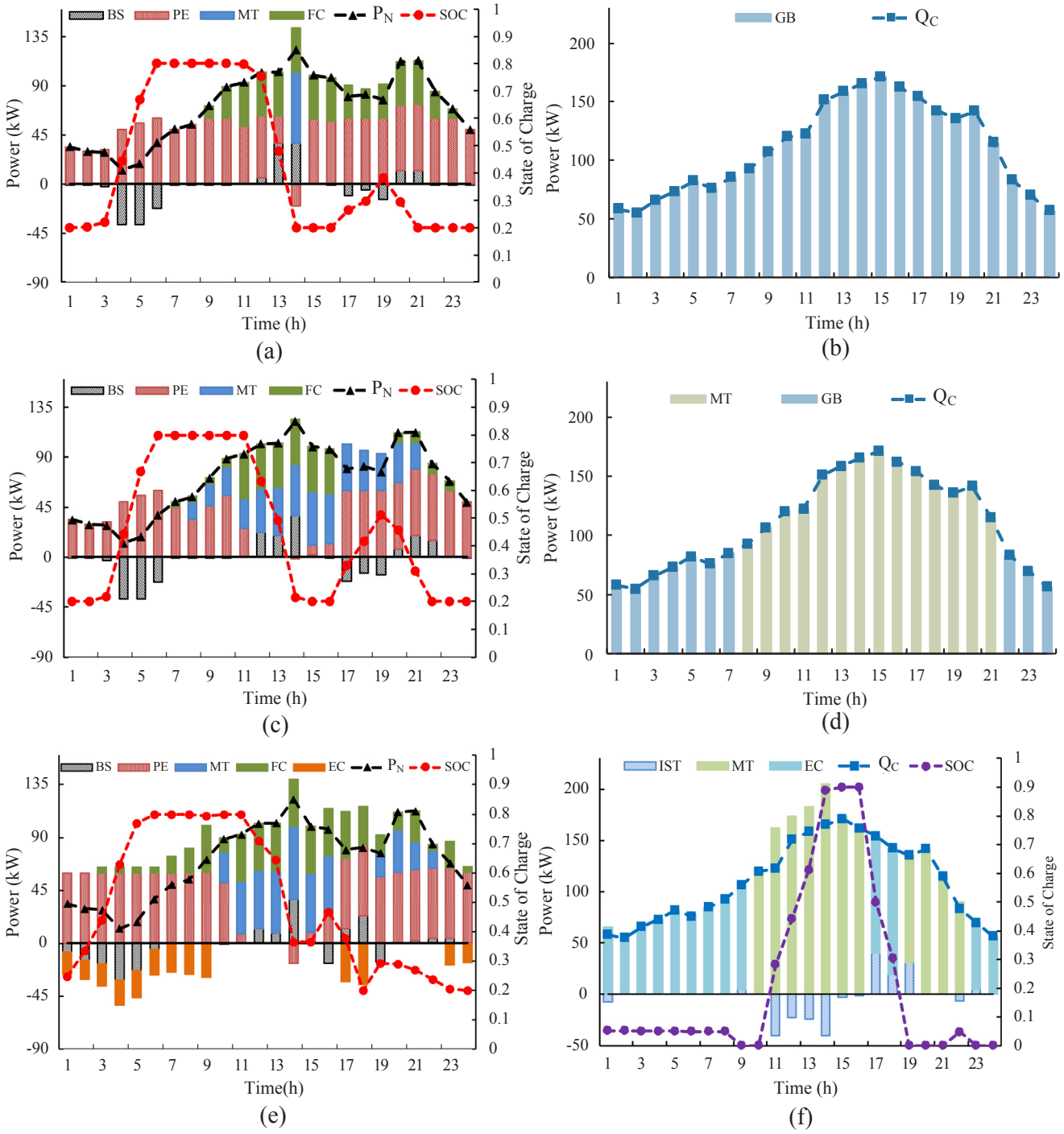

Fig. 6. Power and heat balance conditions of the 3 cases in summer for the grid-connected microgrid. Case 1 (a), (b), Case 2 (c), (d), Case 3 (e), (f).

condition, demand response may be invoked if the energy supply is not enough, *i.e.*, part of loads can be cut off, or part of energy can be abandoned with energy deviation cost to balance the energy when necessary [11,39]. Thus, compared with the grid-connected microgrid, the energy deviation cost (or demand response cost) should be considered in the net operating cost function F_S.

(1) Objective function:

$$MIN\ F_S = C_{CP} + \sum_{t=1}^{N} (C_F^t + C_{OM}^t + C_{ST}^t + C_{SD}^t - C_{SHC}^t + C_{PH}^t)\Delta t \tag{28}$$

(a) Energy deviation cost C_{PH}^t [11]:

$$C_{PH}^t = c_{TS} Q_{TS}^t + c_{TE} Q_{TE}^t + c_{IS} Q_{IS}^t + c_{IE} Q_{IE}^t + c_{DS} P_{DS}^t + c_{DE} P_{DE}^t \tag{29}$$

(b) Revenue of supplying heat and cooling to customers C_{SHC}^t:

$$C_{SHC}^t = C_{SH}^t + C_{SC}^t = c_H(Q_H^t - Q_{TS}^t) + c_C(Q_C^t - Q_{IS}^t) \tag{30}$$

where c_{TE}, c_{IE}, c_{DE} and c_{TS}, c_{IS}, c_{DS} are the unit cost for heat, cooling and power surplus and shortage; C_{SHC}^t and C_{SHC}^t denote the revenue of selling heat and cooling to the local customers in islanded microgrid; Q_{TS}^t,Q_{IS}^t,P_{DS}^t and Q_{TE}^t,Q_{IE}^t,P_{DE}^t denote the heat, cooling and power surplus and shortage; C_{SH}^t and C_{SC}^t denote the heat and cooling selling revenue respectively.

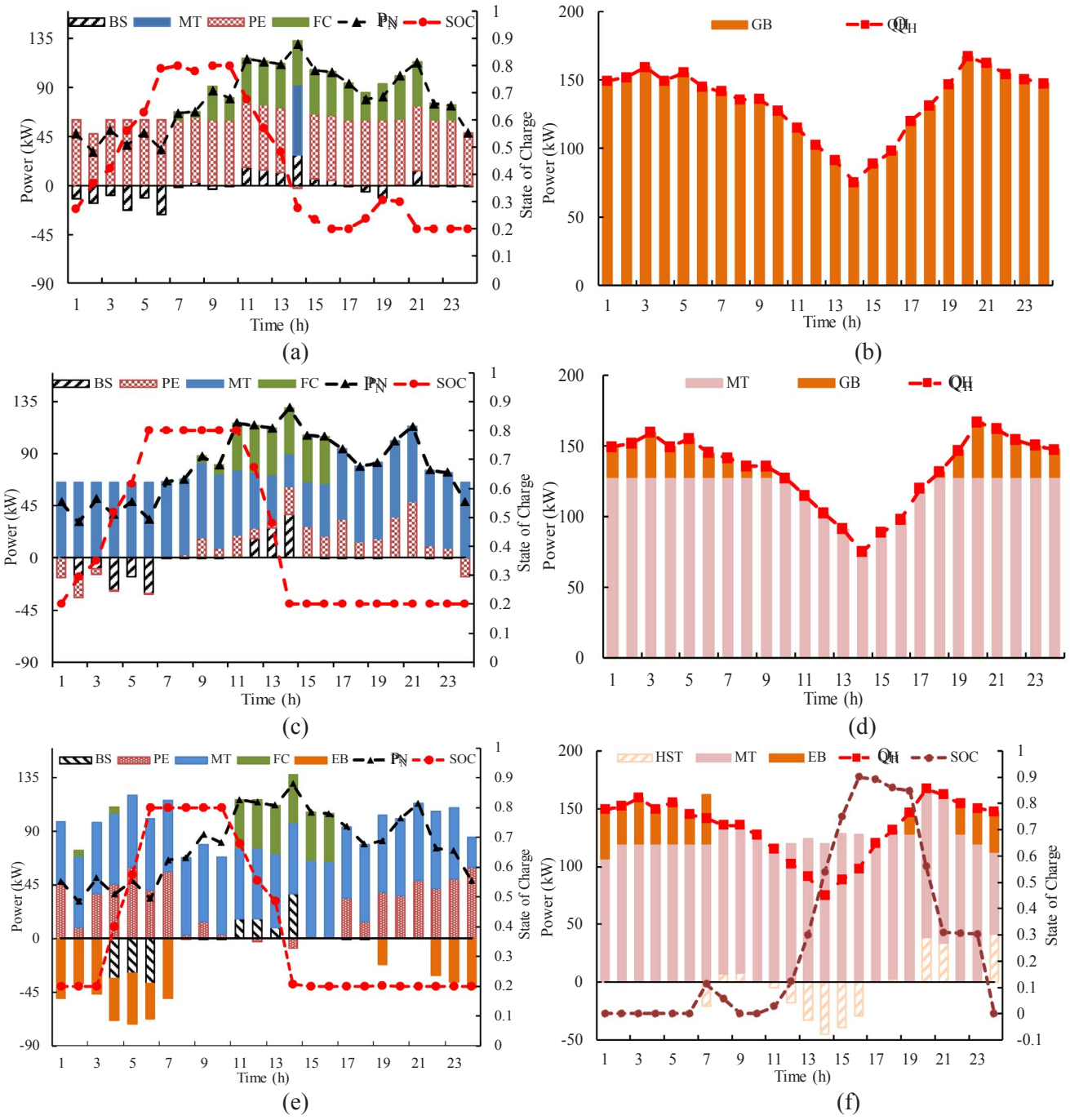

Fig. 7. Power and heat balance conditions of the 3 cases in winter for the grid-connected microgrid. Case 1 (a), (b) Case 2 (c), (d) Case 3 (e), (f).

The cost items with the same symbols have the same meaning and mathematical expressions with the grid-connected mode.

(2) Constraints:

The operational constraints for the islanded microgrid are:

(a) Energy balance:

$$P_{WT}^t + P_{PV}^t + P_{MT}^t + P_{FC}^t + P_{BSD}^t - P_{BSC}^t = P_L^t - P_{DS}^t + P_{DE}^t + P_{EB}^t + P_{EC}^t \tag{31}$$

$$Q_{EC}^t + Q_{MTC}^t - P_{ISTC}^t + P_{ISTD}^t = Q_C^t - Q_{IS}^t + Q_{IE}^t \tag{32}$$

$$Q_{EB}^t + Q_{MTH}^t - P_{HSTC}^t + P_{HSTD}^t = Q_H^t - Q_{TS}^t + Q_{TE}^t \tag{33}$$

(b) Energy deviations:

$$\text{Energy deviation limits: } \begin{cases} 0 \le P_{DS}^t \le \gamma_{DS}^t P_L^t, 0 \le P_{DE}^t \le \gamma_{DE}^t P_L^t \\ 0 \le Q_{TS}^t \le \gamma_{TS}^t Q_H^t, 0 \le Q_{TE}^t \le \gamma_{TE}^t Q_H^t \\ 0 \le Q_{IS}^t \le \gamma_{IS}^t Q_C^t, 0 \le Q_{IE}^t \le \gamma_{IE}^t Q_C^t \end{cases} \tag{34}$$

$$\text{State limits: } \gamma_{DS}^t + \gamma_{DE}^t \le 1, \gamma_{TS}^t + \gamma_{TE}^t \le 1, \gamma_{IS}^t + \gamma_{IE}^t \le 1 \tag{35}$$

where γ_{TS}^t,γ_{IS}^t and γ_{DS}^t are binary indicators of heat, cooling and power shortage when they are equal to 1; with the same definition, γ_{TE}^t,γ_{IE}^t and γ_{DE}^t denote binary indicators of the heat, cooling and power surplus.

Other constraints are in line with the grid-connected microgrid.

Table 5
Net operating cost of grid-connected microgrid (¥).

Cost/revenue item	Summer			Winter		
	Case 1	Case 2	Case 3	Case 1	Case 2	Case 3
Capital cost	671.59	671.59	635.35	671.59	671.59	642.47
Fuel cost	822.70	808.20	685.60	1342.00	1564.30	1507.50
Maintenance cost	77.40	103.60	94.50	88.90	195.00	175.50
Start-up/shut-down cost	9.40	16.10	6.11	9.40	9.80	7.40
Power exchange cost	537.30	350.50	377.60	629.90	177.60	187.80
Heat/cooling revenue	528.40	528.40	528.40	960.10	960.10	960.10
Net operating cost	1590.19	1421.69	1271.05	1781.89	1658.19	1560.77

3.3. Model linearization

Commonly, the linear constant electrical efficiencies of the CCHP plant and FC are utilized to simplify the overall operating problem, *e.g.*, the reference [5,7–10] and [19,20]. However, it is not so accurate to represent their real operational conditions. In practice, the electrical efficiencies are the nonlinear functions of their power outputs with the influence of ambient temperature and elevation [26,40], hence the items with those efficiencies, *i.e.*, the fuel cost function (Eq. (10)), heat/cooling outputs functions (Eqs. (2) and (3)) and the objective functions (Eqs. (8) and (28)) are nonlinear. Besides, it is obvious that the start-up/shut-down cost functions (Eqs. (12) and (13)) are also nonlinear. Thus, the proposed models are regarded as the mixed integer nonlinear programming problems.

To reduce the computation burdens and improve the solution quality, the above nonlinear problems will be linearized into MILP ones.

(1) Linearization of the fuel cost

The fuel cost curves of the CCHP plant and FC can be plotted as the solid line in Fig. 2(a), the heat/cooling outputs curves of the CCHP plant can be plotted as the solid line in Fig. 2(b). N_L blocks of linear functions in dash lines are used to approximate the original nonlinear functions by introducing a binary variable and a continuous variable in each block.

Piecewise-linear functions for the fuel cost and heat/cooling outputs of CCHP plant are

$$\overline{f}(t) = \sum_{k=1}^{N_L} (\alpha_k P_k^t + \beta_k B_k^t) \tag{36}$$

$$\alpha_k = [(f(P_{k+1}) - f(P_k))/(P_{k+1} - P_k)] \tag{37}$$

$$\beta_k = f(P_k) - P_k \alpha_k \tag{38}$$

$$P_k B_k^t \le P_k^t \le B_k^t P_{k+1} \tag{39}$$

$$U_j^t = \sum_{k=1}^{N_L} B_k^t \le 1 \tag{40}$$

where f and $\overline{f}$ are the original and approximated linearized functions; k is the index of the blocks; α_k and β_k denote the slope and intercept of the linear function in block k; P_k is the starting point of kth block, in which P_1 and P_{N+1} in Fig. 2 denote the minimum and maximum power outputs; B_k^t is the binary state of block k.

(2) The linearization of the start-up/shut-down cost can be achieved by separating of the max function into two individual parts as:

$$\begin{cases} C_{ST}^t \ge 0 \\ C_{ST}^t \ge \sum_{j=1}^{N_{CG}} (U_j^t - U_j^{t-1}) C_{ST,j}^U \end{cases} \tag{41}$$

$$\begin{cases} C_{SD}^t \ge 0 \\ C_{SD}^t \ge \sum_{j=1}^{N_{CG}} (U_j^{t-1} - U_j^t) C_{SD,j}^D \end{cases} \tag{42}$$

Then, after the linearization, some commercial solvers like GUROBI and CPLEX which have high performances in solving the MILP problems can be employed.

4. Case studies

4.1. Data input

In this section, the proposed dispatch method is tested in a multi-energy microgrid test system. The hourly power outputs of WT and PV as well as the system loads for the typical winter and summer days can be obtained by forecasting [15,41,42]. The heat and cooling are mainly used for the space heating and cooling in this study. Thus, it is assumed that no heat loads in summer and no cooling loads in winter [18]. The power outputs of WT and PV as well as the system load profiles are shown in Fig. 3. The data are obtained from [12,20,27] and then modified with the practical considerations.

The energy dispatch is conducted for a 24 h horizon with the unit dispatch interval as 1 h. The real-time power pricing scheme shown in Fig. 4 is utilized for the power dispatch [27]. For supplying heat/cooling energy, the fixed pricing scheme is adopted [19]. The parameters for energy storage and DGs are listed in Tables 1 and 2. Other parameters for the case studies are shown in Table 3. Besides, all the units are assumed to be off before the operation [11].

To verify the advantages of the proposed method, two cases based on the conventional energy supplying methods for the microgrids are compared in this paper.

Case 1: Separate generation. Here, the heat/cooling loads are all met by the gas boiler (GB) with heat efficiency of 85% and absorption chiller; the power loads are satisfied by WT, PV, FC, MT, BS and/or demand response [10,19]. In this case, the waste heat is not recovered. Thus MT works only for the power generation.

Case 2: Typical tri-generation. For supplying heat/cooling, the MT (or CCHP plant) operates under FHL strategy in grid-connected microgrid and under FPL strategy in islanded microgrid with GB working as a supplement [15–19,24]. Then the power outputs of MT coordinates with WT, PV, FC, ES and/or demand response to satisfy the system power loads.

Case 3: The system-wide coordinated generation proposed in this paper.

It should be noted that in case 2 and case 3, MT generates power and cooling in summer, while in winter, only power and heat are generated. The detailed combination of the units in the three cases is summarized in Table 4.

The mathematical models are implemented in the General Algebraic Modelling System (GAMS) platform, then the CPLEX solver, which has high performances in solving MILP problems by either the primal variants of simplex method or the barrier interior point method, can be employed [45]. The simulation is run on an Intel(R) Xeon(R) E5-1630 3.70 GHz personal computer with 16 G memory.

4.2. Remarks

To better illustrate the simulation results for the grid-connected microgrid, the unit cost of FC for the power generation $C_{U,FC}^t$ can be calculated as:

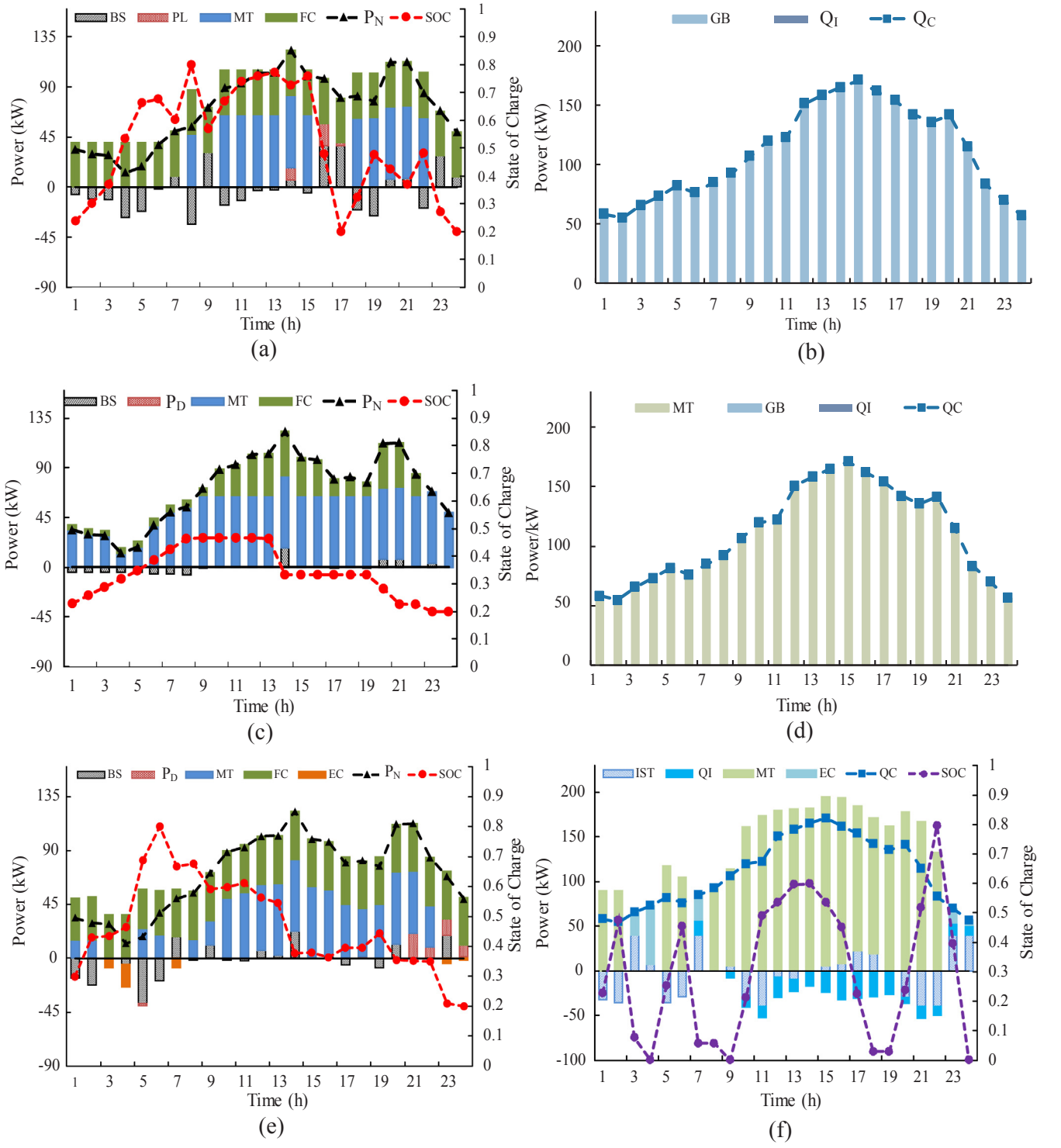

Fig. 8. Power and heat balance condition of the 3 cases in summer for the islanded microgrid. Case 1 (a), (b), Case 2 (c), (d), Case 3 (e), (f).

$$C^t_{U,FC} = C^t_{F,FC}/P^t_{FC} + K^{om}_{FC} \tag{43}$$

Similarly, the unit cost of MT in the only power generation mode, *i.e.*, case 1 $C^t_{U,PG}$ is:

$$C^t_{U,PG} = C^t_{F,MT}/P^t_{MT} + K^{om}_{MT} \tag{44}$$

The unit cost of MT operating in summer $C^t_{U,S}$ and winter $C^t_{U,W}$, *i.e.*, case 2 and 3 is as follows:

$$C^t_{U,W} = (C^t_{F,MT} - c_H Q^t_{MTH})/P^t_{MT} + K^{om}_{MT} \tag{45}$$

$$C^t_{U,S} = (C^t_{F,MT} - c_C Q^t_{MTC})/P^t_{MT} + K^{om}_{MT} \tag{46}$$

Fig. 5 presents the unit cost curves of FC and MT in different cases based on the Eqs. (43)–(46).

As we can see that due to the nonlinear electrical efficiencies, the unit cost of FC is increasing, while the unit cost of MT in different cases is decreasing with the increasing power outputs. For the coefficient of performance of the absorption chiller is higher than that of the heat recovery unit, therefore the unit cost of MT operating in winter is higher than that in summer, but for the recovery of the waste heat, both

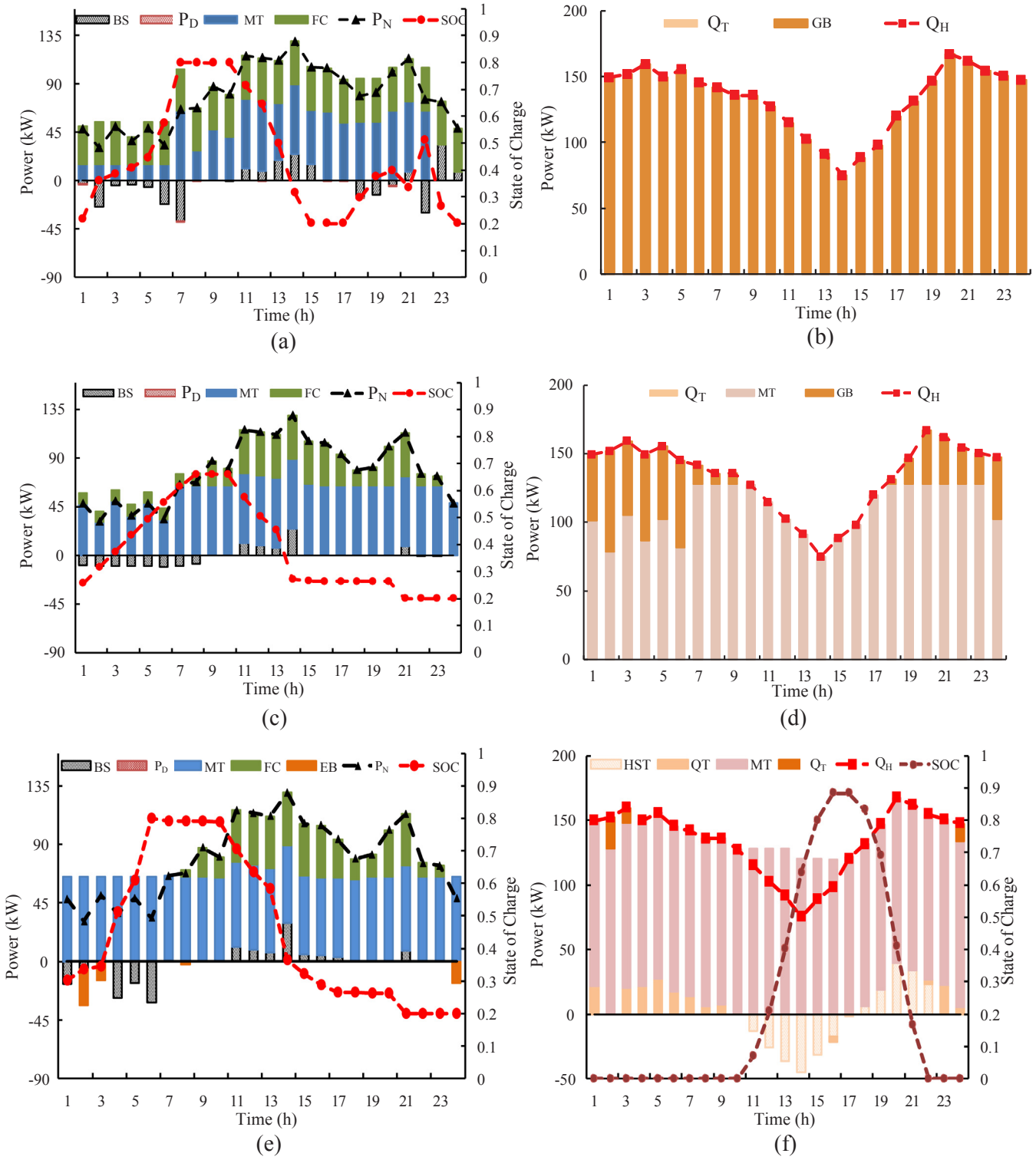

Fig. 9. Power and heat balance conditions of the 3 cases in winter for the islanded microgrid. Case 1 (a), (b), Case 2 (c), (d), Case 3 (e), (f).

costs are lower than that of MT in the only power generation mode, *i.e.*, case 1. In addition, Fig. 5 shows that within FC's maximum capacity, its unit cost is always lower than that of MT in case 1–3.

4.3. Grid-connected mode

Figs. 6 and 7 show the simulation results of the grid-connected microgrid in all three cases. The net operating cost is listed in Table 5. In those figures, P_N denotes the total power loads minus the summation of WT and PV power outputs; PE denotes the subtraction of purchasing power with selling power; BS is the subtraction of discharging power with the charging one. HST and IST denote the subtraction of the releasing heat/cooling energy with the absorbing respectively.

It is indicated in Figs. 6 and 7 that all the units in the three cases are scheduled based on their unit cost as well as the operational constraints. Since the unit power generation cost of FC is lower than MT (Fig. 5), FC outputs in priority when there is power shortage; Except for satisfying the internal power loads, FC and MT will output extra power when their

Table 6
Net operating cost of islanded microgrid (¥).

Cost/revenue item	Summer			Winter		
	Case 1	Case 2	Case 3	Case 1	Case 2	Case 3
Capital cost	671.59	671.59	635.35	671.59	671.59	642.47
Fuel cost	1713.80	1482.40	1254.60	2494.60	1796.10	1671.50
Maintenance cost	208.40	197.80	165.90	231.30	218.40	206.70
Start-up/shut-down cost	15.00	6.40	7.40	7.20	9.80	7.40
Energy deviation cost	50.30	9.00	126.40	0.10	41.10	34.00
Heat/cooling revenue	528.40	528.40	520.10	960.10	960.10	910.70
Net operating cost	2130.79	1838.79	1669.55	2444.69	1776.99	1651.37

unit cost is less than the power selling prices in order to obtain more power exchange revenue. Besides, the charging or discharging decisions of BS are made with respect to the real-time pricing to shift loads and reduce the net operating cost.

In case 1, the heat/cooling loads are all met by GB (Figs. 6(b) and 7(b)), the power loads are supplied by FC, MT, BS and power exchange (Figs. 6(a) and 7(a)) based on their individual cost functions. The simulation results show that the heat/cooling and power are scheduled without any interaction. Since the efficiency of GB is low and the heat generated by MT is all wasted, the net operating cost is the highest (Fig. 6(a) and 7(a), period 14, Table 5).

In case 2, under the FHL strategy, MT supplies heat/cooling in priority and GB works as a supplement (Figs. 6(d) and 7(d)). The fixed power outputs of MT coordinate with FC, BS and the power exchange to satisfy the total power loads (Figs. 6(c) and 7(c)). For the waste heat is fully utilized, the net operating cost is thus lower than case 1 (Table 5). However, under the FHL strategy, MT's power outputs are highly limited by its cooling/heat outputs. Hence MT cannot join in the energy market flexibly and the cost is still high.

By marked contrast, the system-wide optimal coordinated dispatch of power, heat/ cooling is realized in case 3. When the power purchasing prices are lower than the unit cost of MT operating in summer or in winter, the power participates in the heat/cooling dispatch, *i.e.*, EB/EC outputs in priority to MT to transfer the power to heat/cooling (Fig. 6(e) and (f), period 1–9, 17–18, 23–24 and Fig. 7(e) and (f) period 1–7, 22–24). When the power purchasing prices are higher than the unit cost of MT operating in summer or in winter, HST/IST stores the surplus heat/cooling to decouple the inflexible strategies of MT in case 2, then more power can be generated to supply the power loads or be sold to grid for revenue (Fig. 6(e) and (f), period 11–14 and Fig. 7(e) and (f), period 12–17). When the power purchasing prices fall in between the above two price intervals, heat/cooling energy participates in the power dispatch, *i.e.*, HST/IST releases the heat/cooling energy to decrease MT power outputs (Fig. 6(e) and (f), period 17–19 and Fig. 7(e) and (f), period 20–21, 24). Further, it is shown in Fig. 5 that with the increasing power outputs of MT, its unit cost is decreasing, thus, in this way, HST/IST helps MT to fully utilize this advantage to further reduce the net operating cost. Hence, the operating cost of case 3 is the lowest (Table 5).

In summary, the proposed method in this paper can effectively achieve the system-wide coordination for the grid-connected microgrid and reduce its net operating cost.

In terms of the solution speed, all the solutions are obtained within 3.39 s with the minimal solver time is 1.24 s, which is computationally efficient and short enough for the day-ahead dispatch scheme.

4.4. Islanded mode

Simulation results of the microgrid in islanded mode are shown in Figs. 8 and 9. The net operating cost is listed in Table 6. Similarly, P_D, Q_T and Q_I denote the subtraction of power, heat and cooling shortage with their respective energy surplus.

It is shown in Figs. 8 and 9 that since there is no power support from the grid, demand response will be invoked with the energy deviation cost. As shown in Table 3 that the unit power deviation cost is much higher than the unit cost of DGs, thus all the DGs and energy storage are scheduled to reduce power deviations cost.

In case 1, the heat/cooling loads are all met by GB (Figs. 8(b) and 9(b)), the power loads are supplied by FC, MT and BS (Figs. 8(a) and 9(a)). Demand response is invoked only when there is still energy shortage after the maximum power outputs of all the units (Fig. 8(a) period 14, 16–17, Fig. 9(a) period 1, 7, 16–20). Since it costs more for GB to supply heat/cooling and the heat generated by MT is wasted (Figs. 8(a) and 9 (a), period 14), the operating cost is the highest (Table 6).

In case 2, under the FPL strategy, MT supplies the power loads in priority, and if there is still the heat/cooling shortage, GB will start to work as a supplement (Figs. 8(d) and 9(d)). When there is a power imbalance, FC starts to output power and coordinates with BS and demand response if necessary, to satisfy the total power loads (Figs. 8(d) and 9(d)). However, under the FPL strategy, heat/cooling outputs of MT are limited by its power outputs, which hinders its effect in the heat/cooling dispatch. Besides, the power outputs of MT are not generated with regard to its operating cost but only follow the inflexible strategy. Thus, the net operating cost of case 2 is still high (Table 6).

By contrast, case 3 realizes the system-wide coordination between power, heat/cooling in the islanded microgrid, *i.e.*, the power join in the heat/cooling dispatch with the support of EC/EB, MT generates the power and heat/cooling coordinately with the assistance of HST/IST (Figs. 8(e), (f) and 9(e), (f)). Thus, the overall dispatch is more flexible and efficient. Besides, the demand response joins in the overall dispatch according to the energy deviation cost as well which further enhances the dispatch flexibility. The net operating cost of case 3 is still the lowest as the grid-connected case (Table 6).

Furthermore, the maximal solution time for all the islanded microgrid cases is 4.51 s, which again shows the high solution efficiency.

5. Conclusions

This paper proposes a comprehensive system-wide optimal coordinated dispatch method for the multi-energy microgrid in both grid-connected and islanded modes. In the proposed method, HST/IST could decouple the inflexible operational strategies of the CCHP plant and make it join in the power and heat/cooling dispatch with higher flexibility. Besides, EB/EC can significantly enhance the interactions of the dispatch between the power and heat/cooling. Then, comprehensive case studies based on the separate generation, tri-generation and optimal coordinated generation proposed in this paper fully demonstrate that the proposed method can increase the operating efficiency, *i.e.*, reduce the net operating cost as well as achieve more efficient and flexible system operation. It is concluded that the system-wide optimal coordinated dispatch method can provide beneficial references to the design, planning, and operation of the practical multi-energy supplying networks in different modes and have a great potential in further reducing the system net operating cost.

It is also important to note that the proposed method is not limited to a specific microgrid or a specific operating mode for the DGs and energy storage devices. Similar microgrids with multi-energy demands such as the ship microgrid or building microgrid can also be applied [2,46]. For example, a multi-energy microgrid which can be switched between the grid-connected and islanded modes is being built in the Semakau Island of Singapore [4]. Besides, the proposed method will also be implemented on our ship microgrid project with the on-site data [47].

Acknowledgement

The work in this paper is supported by the Singapore Ministry of Education under an Academic Research Fund Tier-1 project. The work of Yan Xu is supported by the Nanyang Assistant Professorship from Nanyang Technological University, Singapore.

References

[1] Mancarella P. MES (multi-energy systems): An overview of concepts and evaluation models. Energy 2014;65:1–17.
[2] Liu M, Shi Y, Fang F. Combined cooling, heating and power systems: A survey. Renewable Sustain Energy Rev 2014;35:1–22.
[3] Cho H, Smith AD, Mago P. Combined cooling, heating and power: A review of performance improvement and optimization. Appl Energy 2014;136:168–85.
[4] NTU to build an offshore integrated system of renewable energy sources; 2016. http://media.ntu.edu.sg/NewsReleases/Pages/newsdetail.aspx?news=830aa91e-aa88-4c7b-8f95-00c171c17560&from=timeline&isappinstalled=0.
[5] Fang F, Wang QH, Shi Y. A novel optimal operational strategy for the CCHP system based on two operating modes. IEEE Trans Power Syst 2012;27(2):1032–41.
[6] Smith AD, Mago PJ. Effects of load-following operational methods on combined heat and power system efficiency. Appl Energy 2014;115:337–51.
[7] Fumo N, Chamra LM. Analysis of combined cooling, heating, and power systems based on source primary energy consumption. Appl Energy 2010;87(6):2023–30.
[8] Fumo N, Mago PJ, Chamra LM. Emission operational strategy for combined cooling, heating, and power systems. Appl Energy 2009;86(11):2344–50.
[9] Kang L, Yang J, An Q, et al. Complementary configuration and performance comparison of CCHP-ORC system with a ground source heat pump under three energy management modes. Energy Convers Manage 2017;135:244–55.
[10] Liu M, Shi Y, Fang F. Optimal power flow and PGU capacity of CCHP systems using a matrix modelling approach. Appl Energy 2013;102:794–802.
[11] Jiang Q, Xue M, Geng G. Energy management of microgrid in grid-connected and stand-alone modes. IEEE Trans Power Syst 2013;28(3):3380–9.
[12] Kanchev H, Colas F, Lazarov V, et al. Emission reduction and economical optimization of an urban microgrid operation including dispatched PV-based active generators. IEEE Trans Sustain Energy 2014;5(4):1397–405.
[13] Meng L, Sanseverino ER, Luna A, et al. Microgrid supervisory controllers and energy management systems: A literature review. Renewable Sustain Energy Rev 2016;60:1263–73.
[14] Moradi MH, Eskandari M, Hosseinian SM. Operational strategy optimization in an optimal sized smart microgrid. IEEE Trans Smart Grid 2015;6(3):1087–95.
[15] Gu W, Wu Z, Bo R, et al. Modelling, planning and optimal energy management of combined cooling, heating and power microgrid: A review. Int J Electr Power Energy Syst 2014;54:26–37.
[16] Ma L, Liu N, Zhang J, et al. Energy management for joint operation of CHP and PV prosumers inside a grid-connected microgrid: A game theoretic approach. IEEE Trans Ind Informat 2016;12(5):1930–42.
[17] Wang L, Li Q, Sun M, et al. Robust optimisation scheduling of CCHP systems with multi-energy based on minimax regret criterion. IET Gener Transm Distrib 2016;10(9):2194–201.
[18] Wang L, Li Q, Ding R, et al. Integrated scheduling of energy supply and demand in microgrids under uncertainty: A robust multi-objective optimization approach. Energy 2017;130(1):1–14.
[19] Yan B, Luh PB, Warner G, et al. Operation and design optimization of microgrids with renewables. IEEE Trans Autom Sci Eng 2017;14(2):573–85.
[20] Z.M. Li, Y. Xu, Dynamic dispatch of grid-connected multi-energy microgrids considering opportunity profit. In: IEEE PES general meeting| conference & exposition, 2017. IEEE; 2017 [in press].
[21] Marzband M, Ghadimi M, Sumper A, et al. Experimental validation of a real-time energy management system using multi-period gravitational search algorithm for microgrids in islanded mode. Appl Energy 2014;128:164–74.
[22] Belvedere B, Bianchi M, Borghetti A, et al. A microcontroller-based power management system for standalone microgrids with hybrid power supply. IEEE Trans Sustain Energy 2012;3(3):422–31.
[23] Marzband M, Sumper A, Ruiz-Álvarez A, et al. Experimental evaluation of a real time energy management system for stand-alone microgrids in day-ahead markets. Appl Energy 2013;106:365–76.
[24] Basu AK, Bhattacharya A, Chowdhury S, et al. Planned scheduling for economic power sharing in a CHP-based micro-grid. IEEE Trans Power Syst 2012;27(1):30–8.
[25] Ferreira RS, Borges CLT, Pereira MVF. A flexible mixed-integer linear programming approach to the AC optimal power flow in distribution systems. IEEE Trans Power Syst 2014;29(5):2447–59.
[26] Rasul MG, Ault C, Sajjad M. Bio-gas mixed fuel micro gas turbine co-generation for meeting power demand in australian remote areas. Energy Procedia 2015;75:1065–71.
[27] Wang MQ, Gooi HB. Spinning reserve estimation in microgrids. IEEE Trans Power Syst 2011;26(3):1164–74.
[28] Zhang C, Xu Y, Dong ZY, et al. Robust coordination of distributed generation and price-based demand response in microgrids. IEEE Trans Smart Grid 2017;3(99):1–12.
[29] Aktas A, Erhan K, Ozdemir S, et al. Experimental investigation of a new smart energy management algorithm for a hybrid energy storage system in smart grid applications. Electr Pow Syst Res 2017;144:185–96.
[30] Luo X, Wang J, Dooner M, et al. Overview of current development in electrical energy storage technologies and the application potential in power system operation. Appl Energy 2015;137(6):511–36.
[31] Zhang C, Xu Y, Dong ZY, et al. Robust operation of microgrids via two-stage coordinated energy storage and direct load control. IEEE Trans Power Syst 2016;5(99):1–10.
[32] "State of Green Company"; 2017. https://stateofgreen.com/en/profiles/ramboll/solutions/heat-accumulator-for-chp-plants.
[33] Choudhury A, Chandra H, Arora A. Application of solid oxide fuel cell technology for power generation—A review. Renew Sustain Energy Rev 2013;20:430–42.
[34] Zhao Z, Lee WC, Shin Y, et al. An optimal power scheduling method for demand response in home energy management system. IEEE Trans Smart Grid 2013;4(3):1391–400.
[35] Laudani A, Fulginei FR, Salvini A. High performing extraction procedure for the one-diode model of a photovoltaic panel from experimental I-V curves by using reduced forms. Sol Energy 2014;103:316–26.
[36] Ma T, Yang H, Lu L. A feasibility study of a stand-alone hybrid solar–wind–battery system for a remote island. Appl Energy 2014;121:149–58.
[37] Basaran K, Cetin NS, Borekci S. Energy management for on-grid and off-grid wind/PV and battery hybrid systems. IET Renew Power Gen 2016;11(5):642–9.
[38] Chen SX, Gooi HB, Wang MQ. Sizing of energy storage for microgrids. IEEE Trans Smart Grid 2012;3(1):142–51.
[39] Wang Q, Zhang C, Ding Y, et al. Review of real-time electricity markets for integrating distributed energy resources and demand response. Appl Energy 2015;138:695–706.
[40] Gadalla M, Zafar S. Analysis of a hydrogen fuel cell-PV power system for small UAV. Int J Hydrogen Energy 2016;41(15):6422–32.
[41] Zhang R, Dong ZY, Xu Y, et al. Short-term load forecasting of Australian National Electricity Market by an ensemble model of extreme learning machine. IET Gener Transm Dis 2013;7(4):391–7.
[42] Tascikaraoglu A, Erdinc O, Uzunoglu M, et al. An adaptive load dispatching and forecasting strategy for a virtual power plant including renewable energy conversion units. Appl Energy 2014;119:445–53.
[43] Chen J, Yang X, Zhu L, et al. Microgrid economic operation and research on dispatch strategy. In: Power engineering and automation conference (PEAM), 2012 IEEE. IEEE; 2012. p. 1–6.
[44] Lv Q, Jiang H, Chen T. Wind power accommodation by combined heat and power plant with electric boiler and its national economic evaluation. Autom Electr Power Syst 2014;38(1):6–12. [in Chinese].
[45] Cplex G. The solver manuals. Gams/Cplex; 2014.
[46] Jayasinghe SG, Meegahapola L, Fernando N, et al. Review of ship microgrids: system architectures, storage technologies and power quality aspects. Invent 2017;2(1):4.
[47] NTU signs strategic R & D partnership with the Norwegian Energy Collaboratorium established in Singapore; 2017. http://erian.ntu.edu.sg/NE/Pages/News-Detail.aspx?news=29a16659-1f78-438b-822d-4f656e81ffde.

Zhengmao Li received the B.E. degree in Electronic Information Engineering in 2013 and the M.E. degree in Electrical Engineering in 2016, all from Shandong University, Ji'nan, China. Currently he is pursuing the Ph.D. degree at the School of Electrical and Electronic Engineering, Nanyang Technological University, Singapore. His research interests include renewable energy sources, future multi-energy systems, combined cooling, heat and power technology, and optimization techniques.

Yan Xu received the B.E. and M.E degrees from South China University of Technology, Guangzhou, China in 2008 and 2011, respectively, and the Ph.D. degree from The University of Newcastle, Australia, in 2013. He is now the Nanyang Assistant Professor with the School of Electrical and Electronic Engineering, Nanyang Technological University, Singapore. He was previously with the School of Electrical and Information Engineering, University of Sydney, Australia. His research interests include power system stability and control, microgrid and multi-energy system, and data-analytics for smart grids.